

Backstepping controller for speed loop of permanent magnet synchronous motors integrated with a time-varying disturbance load observer for Metro Nhon-Hanoi Station

An Thi Hoai Thu Anh¹, Lam Quang Thai², Pham Duc Minh¹

¹Department of Electrical Engineering, Faculty of Electrical-Electronic Engineering, University of Transport and Communications, Hanoi, Vietnam

²Division of Electrical-Electronic Engineering, Campus in Ho Chi Minh City, University of Transport and Communications, Ho Chi Minh, Vietnam

Article Info

Article history:

Received Jun 6, 2024

Revised Aug 22, 2024

Accepted Sep 3, 2024

Keywords:

Backstepping controller

Electric trains

Proportional-integral controller

Permanent magnet synchronous motors

Time-varying disturbance observer

ABSTRACT

Urban rail systems offer the substantial potential for reducing environmental pollution, alleviating traffic congestion, ensuring safety, and maintaining punctuality. Nevertheless, the operation of urban rail demands substantial electrical energy, and saving energy solutions are crucial to exploiting the full advantages of electric trains. This paper proposes the replacement of traditional traction motors with permanent magnet synchronous motors (PMSMs) due to their superior efficiency, reduced power losses, and compact size compared to direct current (DC) motors or other asynchronous three-phase motors with equivalent power, developing a backstepping controller for the speed loop coupled with a load observer-time-varying disturbance (TVD). The simulation results were conducted in MATLAB/Simulink with parameters collected from the Nhon-Hanoi urban railway line, Vietnam, verifying the proposed algorithms' correctness and effectiveness.

This is an open access article under the [CC BY-SA](https://creativecommons.org/licenses/by-sa/4.0/) license.



Corresponding Author:

An Thi Hoai Thu Anh

Department of Electrical Engineering, Faculty of Electrical-Electronic Engineering, University of Transport and Communications

N0 3 Cau Giay, Lang Thuong Commune, Dong Da District, Hanoi, Vietnam

Email: htanh.ktd@utc.edu.vn

1. INTRODUCTION

In recent years, urban rail systems have met the increasing demands of passenger travel, decreased environmental emissions, ensured safety, and enhanced punctual operations. However, these systems consume significant amounts of electrical energy [1]. Therefore, numerous energy-saving strategies have been implemented, such as energy recovery through regenerative braking using supercapacitors located either at substations or on-board, optimizing train schedules for mutual energy exchange among trains, replacing diode rectifiers at traction substations with bidirectional active rectifiers, promoting energy-efficient driving, deploying efficient traction systems, developing optimal speed profiles, and managing energy intelligently [2].

Choosing the appropriate motor type is one of the critical strategies for saving energy. Various motor types, such as linear, induction (IM), direct current (DC), and permanent magnet synchronous motor (PMSM), are considered for electric trains [3]–[6]. PMSM motors are particularly advantageous because they generate high torque, operate quietly, and offer higher efficiency and compactness than other motors of similar power [7], [8]. These attributes make PMSM motors energy-efficient and reduce maintenance costs [9]–[12]. Given their nature as multi-variable, nonlinear, and sensitive systems to parameter and disturbance variations, traditional linear control methods fall short in accurately modelling PMSM systems. Advanced

control methods like max-plus control, multiplier control, neuro-fuzzy control, sliding mode control, and backstepping control have become widely adopted, addressing various system requirements [13], [14]. The backstepping controller is notable for its robust stability, even amidst system noise or parameter variations over time [15]–[19].

The dynamics of a moving train are influenced by more complex and variable forces than those typical of industrial loads. For instance, the train's substantial mass significantly impacts its operation, and passenger load variations between trips further complicate load dynamics. Weather variations also affect traction and movement due to changes in wind force, rail conditions, and adherence during weather conditions like rain, snow, dryness, or storms. Addressing these challenges necessitates a load observer capable of estimating time-varying torque disturbances to enhance system performance and counteract disturbances [20], [21]. Zhao *et al.* have also proposed the model-free adaptive discrete-time integral terminal sliding mode control (MFA-DITSMC) without a model and a nonlinear disturbance observer (NDO) to improve speed control and resist disturbances [22], [23]. In another study, Lan and Lei-Zhou introduced backstepping control for speed loop and disturbance load observer design that tracks speed and manages disturbances [24]. However, these solutions also introduce increased system complexity and exhibit certain limitations. Hence, this paper introduces a backstepping controller (BSC) integrated with a time-varying disturbance (TVD) load observer to better estimate load disturbances along the Nhon-Hanoi Station.

2. MODELING THE ELECTRIFIED TRAIN

Modeling electric trains involves modeling the traction motor and the resistive forces acting on the train. The traction motors are PMSMs with the field-oriented control (FOC) method, and the mathematical equations are represented in the dq coordinate system. The resistive forces include gradient resistance, curve radius resistance, and basic resistance.

2.1. Modeling PMSM motor

The mathematical equations of i_{sd} and i_{sq} are expressed as (1):

$$\begin{cases} \frac{di_d}{dt} = -\frac{1}{T_d} i_{sd} + \omega_e \frac{L_q}{L_d} i_{sq} + \frac{1}{L_q} v_{sd} \\ \frac{di_q}{dt} = -\omega_s \frac{L_d}{L_q} i_{sd} - \frac{1}{T_q} i_{sq} + \frac{1}{L_q} v_{sq} - \omega_e \frac{\psi_p}{L_q} \end{cases} \quad (1)$$

in which ω_e is the rotor speed, i_{sd} and i_{sq} are the stator current on the dq-axis, v_{sd} and v_{sq} are the stator voltages on the dq-axis, L_d and L_q are the stator inductances on the dq-axis, $T_d = \frac{L_d}{R_s}$ và $T_q = \frac{L_q}{R_s}$ is the time constant on the d-q axis, R_s is the stator resistance, ψ_p is the rotor flux linkage. The electromagnetic torque on the d-q coordinate system is:

$$T_e = \frac{3}{2} P_p [\psi_p i_{sq} + (L_d - L_q) i_{sd} i_{sq}] \quad (2)$$

where T_e is the electromagnetic torque, P_p is the number of pole pairs. The motion equation of the motor is written as (3):

$$\frac{J}{P_p} \frac{d\omega}{dt} = T_e - T_l \quad (3)$$

with T_l is the load torque, $J = J_{dc} + J_{eq}$ is the total moment of inertia of the motor and train, $J_{eq} = \frac{1}{4} \frac{M}{N} \left(\frac{D_{wh}}{\tau} \right)^2$: J_{eq} is the moment of inertia of the train, M is the mass of the train, N is the number of motors, D_{wh} is the diameter of the wheels, τ is the transmission ratio.

2.2. Modeling resistance forces against moving trains

The train's resistance includes forces such as air, friction, curvature, and gradient resistance [25]–[27].

$$F_{res} = F_{grad} + F_r + W_o \quad (4)$$

In which: $F_{grad} = mg \sin a$, m (kg) is the mass of the train, g (m/s^2) is the acceleration due to gravity $\sin a = \sin(\arcsin(i_k))$ where $i_k(\frac{\circ}{\circ})$ is the slope, a representing the gradient of the track. $F_r = \frac{A}{R}$, R – minimum curve radius, in meters, A – A coefficient determined experimentally. $W_0 = a + bv + cv^2$, v is the velocity (m/s), the resistance coefficients a (N), b (Ns/m), c (Ns^2/m^2) are experimentally provided by the manufacturer.

3. BACKSTEPPING CONTROL FOR SPEED LOOP

Figure 1 shows the control structure diagram of the electric train drive system based on the rotor flux-oriented control (FOC) combined with control methods in the weak magnetic field area. The control structure includes a speed loop, the i_{sd} current loop, and the i_{sq} current loop. This section primarily focuses on the motor's speed loop.

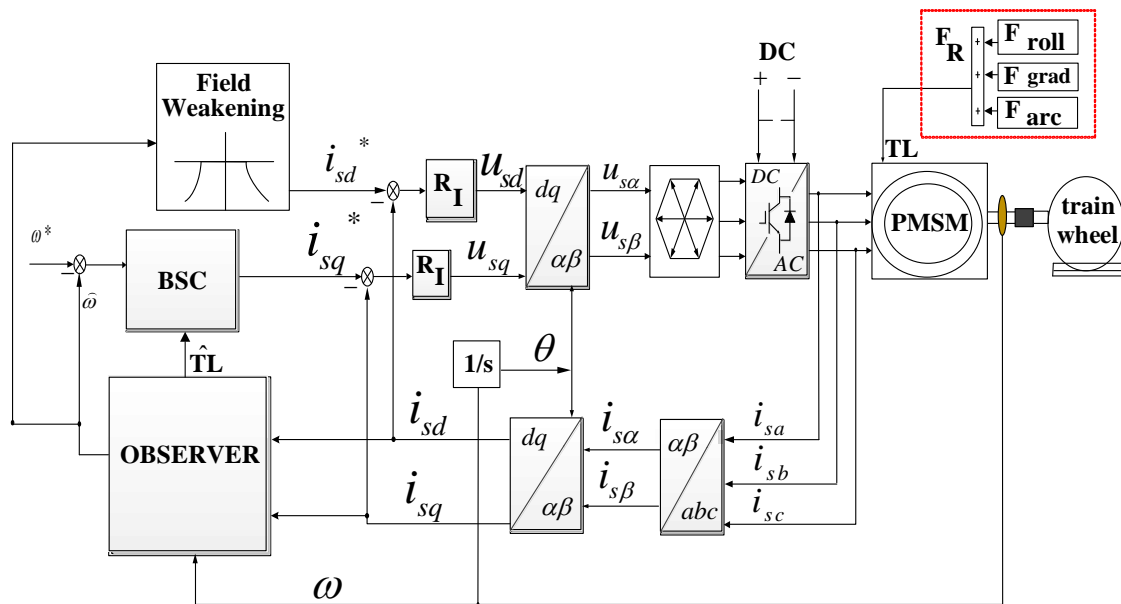


Figure 1. FOC control structure with backstepping control and load observer – TVD

Using the concept of backstepping and Lyapunov system stabilization [28]. Considering speed deviation:

$$e = w^* - w \tag{5}$$

With as the input value and as the actual value, we obtain the derivative of e as (6):

$$\dot{e} = \dot{w}^* - \dot{w} \tag{6}$$

Choose a Lyapunov function for the deviation e:

$$V = \frac{1}{2}e^2 \tag{7}$$

Differentiating equation (7) results in:

$$\dot{V} = e\dot{e} \tag{8}$$

From there, select the control parameter $K_s > 0$ such that:

$$\dot{e} = -K_s e \tag{9}$$

From (9) substituting into (8), we obtain the following:

$$\dot{V} = -K_s e^2 \leq 0 \quad (10)$$

We can see that the derivative satisfies stability according to Lyapunov. From (9), we can rewrite (6) as (11):

$$T_e - T_l + K_s e - \dot{\omega} = 0 \quad (11)$$

Based on (2), the inferred virtual current control signal i_{sq}^* is:

$$i_{sq}^* = \frac{\dot{\omega} + \frac{P_p}{J} T_l - K_s e}{\frac{3P^2 p}{2J} [\psi_p + (L_d - L_q) i_{sd}]} \quad (12)$$

4. DESIGN OF TIME-VARYING DISTURBANCE OBSERVER

The presence of disturbance in the load torque can reduce control efficiency, so compensation is required in the control system to ensure accuracy. The general equation describing the system of the TVD observer is presented:

$$\dot{x} = au - d \quad (13)$$

With being the measurable signal, the control signal, d the indeterminable disturbance signal.

To achieve this, from the motion equation at (3) and the electromagnetic torque equation, a time-varying disturbance observer can be constructed to estimate and then compensate for disturbances in the (12). From (13), we design the observer in the following form:

$$\begin{cases} \dot{\hat{T}}_l = k_1(\hat{\omega} - \omega) \\ \dot{\hat{\omega}} = -\hat{T}_l + a \cdot i_q - k_2(\hat{\omega} - \omega) \end{cases} \quad (14)$$

With $\hat{T}_l, \hat{\omega}$ as the estimated values T_l, ω , $a = \frac{3}{2} P_p [\psi_p + (L_d - L_q) i_{sd}]$.

Prove stability according to the Lyapunov equation:

$$V = \frac{1}{2k_1} \tilde{d}^2 + \frac{1}{2} \tilde{\omega}^2 \Rightarrow \dot{V} = \frac{1}{k_1} \tilde{d} \dot{\tilde{d}} + \tilde{\omega} \dot{\tilde{\omega}} = \frac{1}{k_1} \tilde{d}(\dot{d} - \dot{\hat{d}}) + \tilde{\omega}(\dot{\omega} - \dot{\hat{\omega}}) \quad (15)$$

With

$$\frac{1}{k_1} \dot{\tilde{d}} \approx 0, \tilde{d} = d - \hat{d}, \tilde{\omega} = \omega - \hat{\omega} \quad (16)$$

Therefore, we have:

$$\dot{V} = \frac{1}{k_1} \tilde{d} \dot{\tilde{d}} + \tilde{\omega} \dot{\tilde{\omega}} = \frac{1}{k_1} \tilde{d}(\dot{d} - \dot{\hat{d}}) + \tilde{\omega}(\dot{\omega} - \dot{\hat{\omega}}) \quad (17)$$

Let's assume \dot{d} limit >0 , k_1 relatively large value, $k_2 >0$

$$\frac{1}{k_1} \dot{\tilde{d}} \approx 0 \quad (18)$$

From the above equations, the following is obtained:

$$\dot{V} = \frac{1}{k_1} \tilde{d} \dot{\tilde{d}} - \frac{1}{k_1} \tilde{d} \dot{\hat{d}} + \tilde{\omega}(\dot{\omega} - (\dot{\hat{d}} + a \cdot i_q - k_2(\hat{\omega} - \omega))) \quad (19)$$

$$\dot{V} = \frac{1}{k_1} \tilde{d} \dot{\tilde{d}} - \frac{1}{k_1} \tilde{d} k_1(\hat{\omega} - \omega) + \tilde{\omega}(a \cdot i_q - d - (-\dot{\hat{d}} + a \cdot i_q - k_2(\hat{\omega} - \omega))) \quad (20)$$

$$\dot{V} = \frac{1}{k_1} \tilde{d} \dot{\tilde{d}} - \tilde{d}(\hat{\omega} - \omega) + \tilde{\omega}(-d + \dot{\hat{d}} - k_2(\hat{\omega} - \omega)) \quad (21)$$

$$\dot{V} = \frac{1}{k_1} \tilde{d}\dot{d} + \tilde{d}\tilde{\omega} + \tilde{\omega}(-\tilde{d} - k_2\tilde{\omega}) \quad (22)$$

$$\dot{V} = \frac{1}{k_1} \tilde{d}\dot{d} - k_2\tilde{\omega}^2 \leq 0 \text{ Because } \frac{1}{k_1} \tilde{d}\dot{d} \approx 0 \quad (23)$$

5. RESULTS AND DISCUSSION

The Nhon – Ha noi line has a total length of 12.5 km with 12 stations, including 4 underground and 8 above-ground stations. The total travel time from Nhon to Ha Noi station for a four-carriage train is 890.4 seconds (excluding stoppage time). During this journey, the total estimated stoppage time is 285 seconds. This study selects the route from Hà Noi station to Van Mieu station for simulation with a 60 km/h speed, operating 3 phases: Accelerating, coasting, and braking. The simulation parameters collected from the Metro Nhon – Hanoi are shown in Table 1 and Table 2.

Table 1. Parameters of the PMSM motor

Parameters		Value
Rated power	P_{dm}	185 kW
Rated voltage	U_{dm}	525 V
Rated torque	M_{dm}	836 Nm
Stator resistance	R_s	39.224 mΩ
Axis Inductance d	L_d	1.997 mΩ
Axis Inductance q	L_q	5.499 mΩ
Magnet field	ψ	0.5968 Wb
Number of poles	Zp	3
Frequency	f	120 Hz

Table 2. Parameters of the train

Parameters	Unit	Value
Train Setup	2M2T	
Loaded train mass (M)	[kg]	192.000
Number of motors (N)		12
Maximum speed (v_{max})	[km/h]	60
Base speed (v_b)	[km/h]	40
Acceleration when running (0-40 km/h)	[m/s ²]	0.83
Acceleration when running (0-80 km/h)	[m/s ²]	≥ 0.5
Maximum deceleration during normal braking	[m/s ²]	≥ 1
Maximum deceleration during emergency braking	[m/s ²]	≥ 1.25
Resistance coefficient a	[KN]	0.0115070
Resistance coefficient b	[kg/s]	0.0003494
Resistance coefficient c	[kg/m]	0.00005497
Wheel diameter (D_{wh})	[m]	0.84
Transmission ratio (i)		9.5:1
Gearbox efficiency (η_{mech})		0.9
Motor efficiency (η_{em})		0.95
Train inertia (Je_q)	[kg. m ²]	31.272

Figure 2 shows that the speed loop circuit using the backstepping controller effectively controls the speed, maintaining stability without oscillation. This demonstrates the controller's high precision, even when speed changes and time-varying disturbances occur. In Figures 3(a) and 3(b), during the phase from 0 to 18 seconds, when the speed is within the rated range, the torque is constant, and the power is gradually increasing due to the high-power demand in the initial stage. After this phase, the torque curve forms a hyperbola when the motor operates in the flux-weakening region, and the power curve remains constant. From the 20th to the 40th second, during the coasting phase, the source is disconnected, and both the torque and power curves return to zero. During the braking phase, as the train approaches the station, both torque and power are negative, indicating that the traction motor works as a generator during braking, returning energy to the grid.

In Figure 4, the initial phase from 0-the 2nd second, there is a slight deviation between the estimated and actual torque. However, after this period, the estimated torque closely follows the actual torque. This demonstrates the high accuracy and stability of the disturbance observer, even when the load torque changes over time. Towards the end, around the 55th to 58th second, there is a small discrepancy between the load and estimated torque. This is because the electric train is transitioning to a stop state, experiencing a decrease in

speed and encountering resistance forces, causing the observer to lag in adaptation. Overall, the Time-varying Disturbance observer can accurately estimate the load torque during stable operation, requiring only a short time to adjust its estimation in response to rapid changes or significant noise. This highlights the importance of designing an observer capable of quickly adapting to dynamic changes in operation, especially in applications requiring high accuracy and rapid response, like urban electric trains.

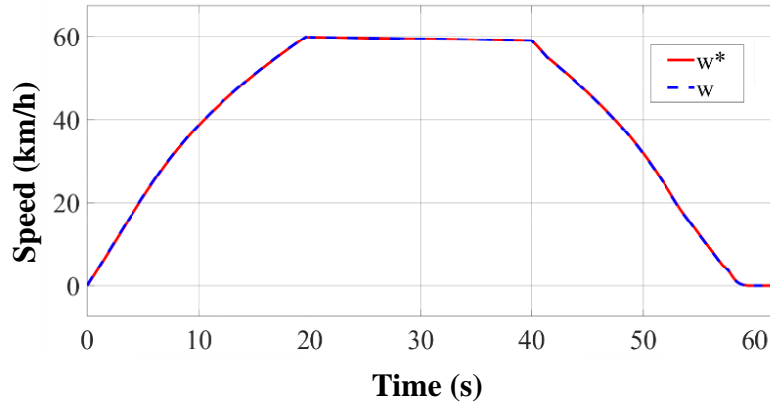
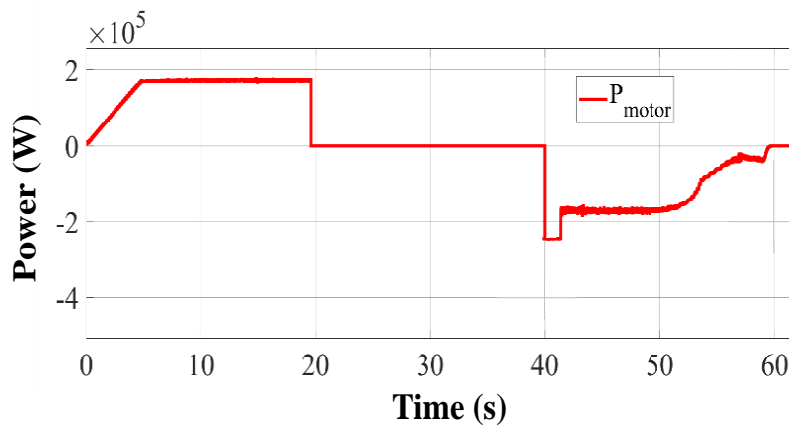
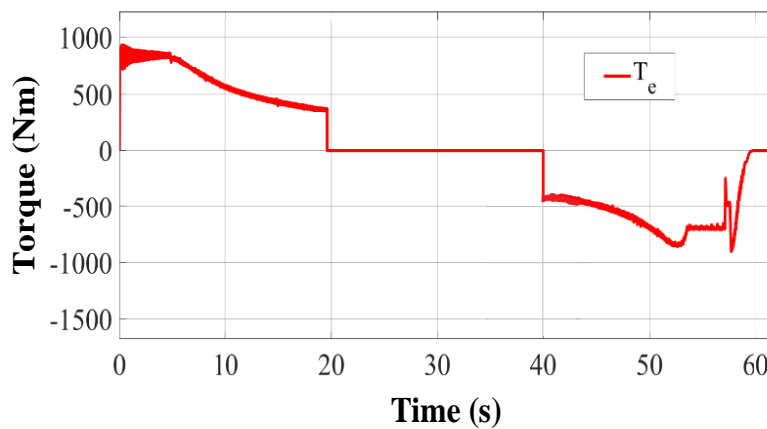


Figure 2. The speed response using backstepping



(a)



(b)

Figure 3. Power, torque responses of electrified train drive system (a) power response and (b) torque response

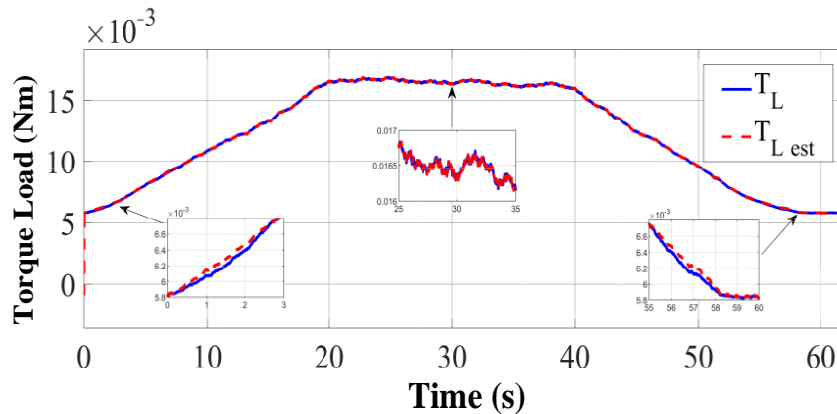


Figure 4. The comparison of the observed torque with the actual torque

6. CONCLUSION

This study proposed a backstepping control method for the speed loop while integrating a time-varying disturbance observer to enhance the ability to monitor load variations and the system's stability. We observed stable speed control and precise tracking of reference signals by employing the backstepping control method for the speed loop. This is crucial in electric train applications where high precision control directly affects schedules and passenger safety. The time-varying disturbance observer, with its ability to detect and adjust to changes over time, helps the control system respond to continuous disturbances. Combined with the backstepping control method, it allows the system to maintain good performance even in the presence of factors causing disturbances, such as changes in load due to fluctuating passenger numbers or other external factors.

REFERENCES

- [1] B. Jin, S. Yang, Q. Wang, and X. Feng, "Study on energy-saving train trajectory optimization based on coasting control in metro lines," *Journal of Advanced Transportation*, vol. 2023, 2023, doi: 10.1155/2023/1217352.
- [2] A. González-Gil, R. Palacin, P. Batty, and J. P. Powell, "A systems approach to reduce urban rail energy consumption," *Energy Conversion and Management*, vol. 80, pp. 509–524, 2014, doi: 10.1016/j.enconman.2014.01.060.
- [3] J. Wang, C. Ren, Z. Liu, and M. Mao, "Research on direct drive technology of the permanent magnet synchronous motor for urban rail vehicles," *Mathematical Problems in Engineering*, vol. 2022, 2022, doi: 10.1155/2022/8312121.
- [4] M. Rezal and D. Ishak, "Performance evaluation of multi-phase permanent magnet synchronous motor based on different winding configurations and magnetization patterns," *International Journal of Power Electronics and Drive Systems*, vol. 10, no. 3, pp. 1197–1206, 2019, doi: 10.11591/ijpeds.v10.i3.pp1197-1206.
- [5] J. Holtz, "Sensorless control of induction motor drives," in *Proceedings of the IEEE*, 2002, vol. 90, no. 8, pp. 1359–1394, doi: 10.1109/JPROC.2002.800726.
- [6] S. Kamar *et al.*, "Performance analysis of three-phase induction motor for railway propulsion system," *International Journal of Power Electronics and Drive Systems*, vol. 14, no. 3, pp. 1433–1441, 2023, doi: 10.11591/ijpeds.v14.i3.pp1433-1441.
- [7] N. Limsuwan, Y. Shibukawa, D. D. Reigosa, and R. D. Lorenz, "Novel design of flux-intensifying interior permanent magnet synchronous machine suitable for self-sensing control at very low speed and power conversion," *IEEE Transactions on Industry Applications*, vol. 47, no. 5, pp. 2004–2012, 2011, doi: 10.1109/TIA.2011.2161534.
- [8] J. M. Crider and S. D. Sudhoff, "An inner rotor flux-modulated permanent magnet synchronous machine for low-speed high-torque applications," *IEEE Transactions on Energy Conversion*, vol. 30, no. 3, pp. 1247–1254, 2015, doi: 10.1109/TEC.2015.2412547.
- [9] H. Douglas, C. Roberts, S. Hillmanssen, and F. Schmid, "An assessment of available measures to reduce traction energy use in railway networks," *Energy Conversion and Management*, vol. 106, pp. 1149–1165, 2015, doi: 10.1016/j.enconman.2015.10.053.
- [10] H. Douglas, F. Schmid, C. Roberts, and S. Hillmanssen, "Evaluation of permanent magnet motor energy saving technology for different types of railways," in *2016 IEEE International Conference on Intelligent Rail Transportation, ICIRT 2016*, 2016, pp. 123–129, doi: 10.1109/ICIRT.2016.7588721.
- [11] K. Kondo, "Recent energy saving technologies on railway traction systems," *IEEJ Transactions on Electrical and Electronic Engineering*, vol. 5, no. 3, pp. 298–303, 2010, doi: 10.1002/tee.20533.
- [12] T. D. Chuyen, V. H. Nguyen, P. N. Dao, N. A. Tuan, and N. Van Toan, "Sliding mode control strategy based lead screw control design in electromechanical tracking drive system," *International Journal of Power Electronics and Drive Systems*, vol. 13, no. 1, pp. 150–158, 2022, doi: 10.11591/ijpeds.v13.i1.pp150-158.
- [13] E. Sabouni, B. Merah, and I. K. Bousserhane, "Adaptive backstepping controller design based on neural network for pmsm speed control," *International Journal of Power Electronics and Drive Systems*, vol. 12, no. 3, pp. 1940–1952, 2021, doi: 10.11591/ijpeds.v12.i3.pp1940-1952.
- [14] Q. Song, Y. D. Song, and W. Cai, "Adaptive backstepping control of train systems with traction/braking dynamics and uncertain resistive forces," *Vehicle System Dynamics*, vol. 49, no. 9, pp. 1441–1454, 2011, doi: 10.1080/00423114.2010.520084.
- [15] W. W. Hager, "Multiplier methods for nonlinear optimal control," *SIAM Journal on Numerical Analysis*, vol. 27, no. 4, pp. 1061–1080, 1990, doi: 10.1137/0727063.

- [16] B. K. Singh and A. Kumar, "Backstepping approach based controller design for magnetic levitation system," in *2018 5th IEEE Uttar Pradesh Section International Conference on Electrical, Electronics and Computer Engineering, UPCON 2018*, 2018, pp. 1–6, doi: 10.1109/UPCON.2018.8596885.
- [17] J. Yan, H. Wang, S. Huang, and Y. Lan, "Disturbance observer-based backstepping control of PMSM for the mine traction electric locomotive," *Mathematical Problems in Engineering*, vol. 2018, 2018, doi: 10.1155/2018/7253210.
- [18] A. Ganapathy Ram and K. R. Santha, "Review of sliding mode observers for sensorless control of permanent magnet synchronous motor drives," *International Journal of Power Electronics and Drive Systems*, vol. 9, no. 1, pp. 46–54, 2018, doi: 10.11591/ijpeds.v9.i1.pp46-54.
- [19] T. Wang, J. Li, and Y. Liu, "Synergetic control of permanent magnet synchronous motor based on load torque observer," in *Proceedings of the Institution of Mechanical Engineers. Part I: Journal of Systems and Control Engineering*, 2019, vol. 233, no. 8, pp. 980–993, doi: 10.1177/0959651818811253.
- [20] Q. Wang, H. Yu, M. Wang, and X. Qi, "An improved sliding mode control using disturbance torque observer for permanent magnet synchronous motor," *IEEE Access*, vol. 7, pp. 36691–36701, 2019, doi: 10.1109/ACCESS.2019.2903439.
- [21] H. K. Khalil, "Extended high-gain observers as disturbance estimators," *SICE Journal of Control, Measurement, and System Integration*, vol. 10, no. 3, pp. 125–134, 2017, doi: 10.9746/jcmsi.10.125.
- [22] X. Zhang, L. Sun, K. Zhao, and L. Sun, "Nonlinear speed control for PMSM system using sliding-mode control and disturbance compensation techniques," *IEEE Transactions on Power Electronics*, vol. 28, no. 3, pp. 1358–1365, 2013.
- [23] Y. Zhao, X. Liu, H. Yu, and J. Yu, "Model-free adaptive discrete-time integral terminal sliding mode control for PMSM drive system with disturbance observer," *IET Electric Power Applications*, vol. 14, no. 10, pp. 1756–1765, 2020, doi: 10.1049/iet-epa.2019.0966.
- [24] Y. H. Lan and Lei-Zhou, "Backstepping control with disturbance observer for permanent magnet synchronous motor," *Journal of Control Science and Engineering*, vol. 2018, 2018, doi: 10.1155/2018/4938389.
- [25] N. D. T. Do Duc Tuan, "Developing a program to calculate the unitresultant force of trains on Vietnam railways," *Transport and Communications Science Journal*, vol. 71, no. 8, pp. 907–923, 2020.
- [26] N. Van Tiem, "Speed control for the train of urban railway using fuzzy-d controller," *Transport and Communications Science Journal*, vol. 71, no. 6, pp. 640–650, 2020.
- [27] N. D. K. T. Van Khoi, "Optimal planning of substations on urban railway power supply systems using integer linear programming," *Transport and Communications Science Journal*, vol. 70, no. 4, pp. 264–278, 2019.
- [28] C. Pukdeboon, "A review of fundamentals of Lyapunov theory," *The Journal of Applied Science*, vol. 10, no. 2, pp. 55–61, 2011.

BIOGRAPHIES OF AUTHORS



An Thi Hoai Thu Anh    received her Engineer (1997), and M.Sc. (2002) degrees in Industrial Automation Engineering from Hanoi University of Science and Technology; and completed PhD degree in 2020 from the University of Transport and Communications (UTC). Now, she is a lecturer at the Faculty of Electrical and Electronic Engineering at the University of Transport and Communications (UTC). Her interests include power electronic converters, electric motor drives, and energy-saving solutions for industry and transportation. She can be contacted by email: htanh.ktd@utc.edu.vn.



Lam Quang Thai    received his Engineer (2018) degrees in Control Engineering and Automation from the University of Transport and Communications (UTC), and completed Master of Science (MSc) in 2021 from the Ho Chi Minh City University of Technology and Education (HCM-UTE) in Electrical Engineering. Now, he is a lecturer in the Department of Electrical and Electronics Engineering at the University of Transport and Communications – Campus in Ho Chi Minh City (UTC2), Vietnam. His current interests include automation control solutions applied for industry and transportation, renewable energy, artificial intelligence (AI). He can be contacted by email: thailq_ph@utc.edu.vn.



Pham Duc Minh    is a fourth-year student majoring in Electrical Engineering at the University of Transport and Communications (UTC), Vietnam. His current interests include power electronics control and electric drive control, which are applied in the transportation and industry. He can be contacted by email: minh201503809@lms.utc.edu.vn.